Organic LETTERS

Letter

pubs.acs.org/OrgLett

Corannulene–Helicene Hybrids: Chiral π-Systems Comprising Both Bowl and Helical Motifs

Takao Fujikawa,[†] Dorin V. Preda,[‡] Yasutomo Segawa,[†,§] Kenichiro Itami,[†,§,∥] and Lawrence T. Scott*[,‡]

[†]Graduate School of Science, Nagoya University, Chikusa, Nagoya 464-8602, Japan

[‡]Merkert Chemistry Center, Boston College, Chestnut Hill, Massachusetts 02467-3860, United States

[§]JST, ERATO, Itami Molecular Nanocarbon Project, Chikusa, Nagoya 464-8602, Japan

[∥]Institute of Transformative Bio-Molecules (WPI-ITbM), Nagoya University, Chikusa, Nagoya 464-8602, Japan

Supporting Information

ABSTRACT: Two distinct structural elements that render π-systems nonplanar, i.e., geodesic curvature and helical motifs, have been combined into new polyarenes that contain both features. The resultant corannulene–[n]helicenes (n = 5, 6) show unique molecular dynamics in their enantiomerization processes, including inversion motions of both the bowl and the helix. Optical resolution of a corannulene-based skeletally chiral molecule was also achieved for the first time, and the influence of the bowl-motif annulation on the chiroptical properties was investigated.

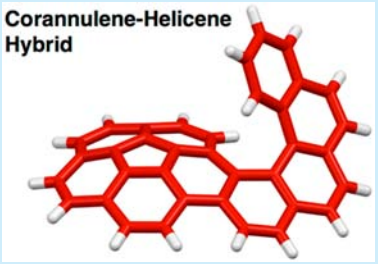

Corannulene, the smallest geodesic (bowl-shaped) polyarene, consisting of five radially fused benzene rings, occupies a venerated position among nonplanar π-systems.[1,2] Notable properties of this simple trigonal-carbon framework include high electron-accepting ability, facile bowl-to-bowl inversion dynamics, and unique chemical reactivity.[3] Although many π-extended corannulenes have been synthesized,[2e,f] skeletally chiral corannulene derivatives have been little-studied. The corannulene cyclotrimer reported by Sygula (**1**) (Figure 1a, left) is one of the rare examples, with three [5]helicene fjord regions and three distinct corannulene moieties, each of which has a different bowl-to-bowl inversion barrier.[4] We also reported that warped nanographene (**2**) (Figure 1a, right), a new class of nanocarbon, exhibits chirality due to the presence of five helical hexa[7]-circulene moieties centered on a corannulene core.[5] In that study, wavelike dynamics of a chiral nanographene with multiple odd-membered-ring defects was demonstrated in solution. As in these molecules, the incorporation of a helical motif endows a corannulene core with skeletal chirality and provides unforeseen molecular behavior. To our surprise, however, no simple chiral corannulene fused with just a single helical motif has ever been reported.

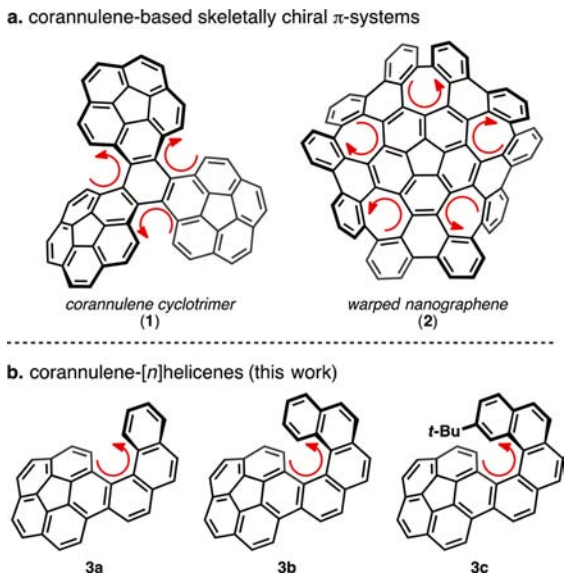

Figure 1. Corannulene-based skeletally chiral π-systems.

Helicenes are helical *ortho*-fused polycyclic aromatic compounds whose π-electron systems are characterized by nonplanarity, large optical rotations, and dynamic behavior.[6] To modulate such properties, π-extension of helical motifs is an effective strategy and has become a recent trend.[7] Nevertheless, it is still unclear how bowl annulation affects helical π-systems. Thus, we were motivated to explore the properties and behavior of the prototype corannulene–[n]helicenes **3a–c** (Figure 1b).

For the synthesis of corannulene–[n]helicenes, we selected formyl corannulene (**4**) as a bowl-shaped starting material and employed photocyclizations to construct the helicene moieties. Wittig reactions of **4** with ylides derived from phosphonium salts **5a–c** afforded the corresponding stilbenes **6a–c** (Scheme 1). Subsequent photocyclization of **6a–c** successfully furnished the target corannulene–[n]helicenes, where n = 5 for **3a** and 6 for **3b** and **3c**. For steric reasons, presumably, a structural isomer **7a** was also produced during the photocyclization of **6a** (**3a**:**7a** = 3:2).

Received: June 20, 2016
Published: August 4, 2016

DOI: 10.1021/acs.orglett.6b01801
Org. Lett. 2016, 18, 3992–3995

Scheme 1. Synthesis of Corannulene−[*n*]Helicenes

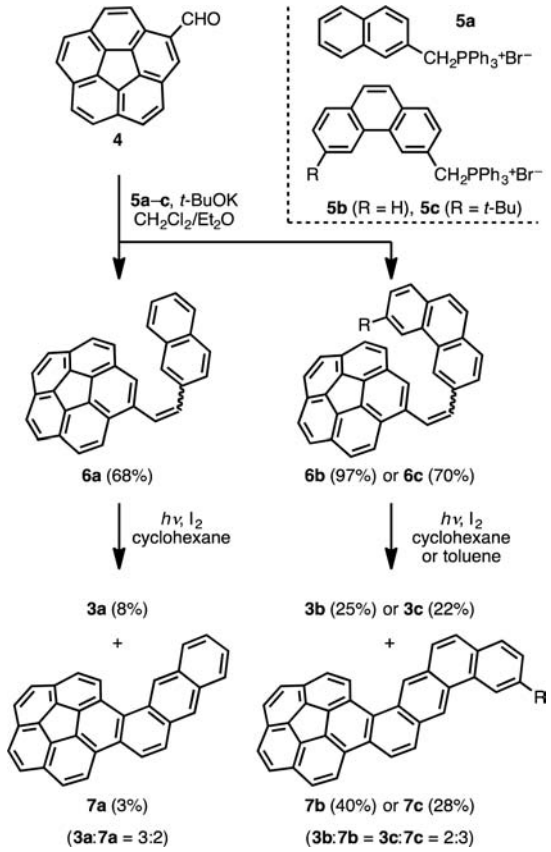

The formation of **7a** was unexpected, because few examples are known to involve photocyclization at the less reactive β-position of a naphthalene onto a large polyarene composed of three or more fused benzene rings.[8] In the photocyclizations of **6b** and **6c**, structural isomers **7b** and **7c** were the dominant products (**3b**:**7b** = **3c**:**7c** = 2:3). The greater steric congestion during [6]helicene formation probably accounts for the observed partitioning.

An important aspect of the structures of corannulene−[*n*]helicenes is the existence of two diastereomeric forms. The terminal ring of the helicene can face either the convex or concave surface of the bowl. Helix inversion results in *P* and *M* helicenes, producing four stereoisomers in total (*convex-P*, *concave-P*, *convex-M*, and *concave-M*).

X-ray crystallographic analysis of a racemic single crystal of **3b** confirmed the distortion caused by the combination of the bowl and the helix, with the molecule adopting a *convex* form (Figure 2). Structural parameters of the two crystallographically independent molecules of *convex*-**3b** in the crystal and the two parent molecules, corannulene and [6]helicene, are listed in Table 1. While corannulene has a C_{5v}-symmetric structure, the X-ray crystal structure of *convex*-**3b** shows significant bond length changes. For example, the rim bond *a*, which is annulated with the helical motif, is greatly lengthened to 1.439(3)/1.437(3) Å compared with 1.383 Å for that of corannulene. The flank bonds *b* and *d* and the hub bond *c* were also lengthened slightly. The sum of the four dihedral angles calculated from the four inner carbon atoms of the [6]helicene moiety of *convex*-**3b** (96.8°/93.8°) was larger than that of [6]helicene (86.8°). For the dihedral angles individually, those near the termini of the helix (*d* and *g*) are increased and those in the middle of the helix (*e* and *f*) are decreased relative to the ones in [6]helicene.

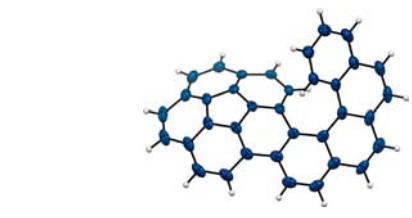

Figure 2. X-ray crystal structure of **3b**. The ORTEP drawing of one of two crystallographically independent molecules (*convex-P*-**3b**) is shown with 50% probabilities.

Table 1. Structural Parameters of the X-ray Crystal Structures of Corannulene,[9] [6]Helicene,[10] and 3b[a]

	corannulene	[6]helicene	**3b**
bond *a* (Å)	1.383	–	1.439(3)/1.437(3)
bond *b* (Å)	1.446	–	1.460(3)/1.462(4)
bond *c* (Å)	1.415	–	1.429(3)/1.430(3)
bond *d* (Å)	1.446	–	1.473(3)/1.477(3)
dihedral *d*	–	15.2°	27.4(3)°/26.4(3)°
dihedral *e*	–	30.3°	25.9(3)°/24.2(3)°
dihedral *f*	–	30.0°	24.8(3)°/25.3(3)°
dihedral *g*	–	11.3°	18.7(3)°/17.9(3)°

[a]Bond lengths *a*–*d* for the X-ray structure of corannulene are averaged values. Dihedral angles were calculated using four consecutive inner carbon atoms inside the helix.

The frozen structure of **3b** in the crystal is fixed in a *convex* conformation, but it is expected to be flexible in solution. Hence, to estimate the dynamic behavior of corannulene−[*n*]helicenes, density functional theory (DFT) calculations at the B3LYP/6-31G(d) level were performed on both the *convex* and *concave* forms of **3a** and **3b** and the transition states for the bowl and helix inversions. Substantial disparities between the thermodynamic stabilities of the *convex* and *concave* conformations were found; *convex*-**3a** is more stable than *concave*-**3a** by 7.5 kcal·mol^{-1}, and *convex*-**3b** is more stable than *concave*-**3b** by 6.3 kcal·mol^{-1}. These results clearly derive from the differences in steric congestion between the two forms. For example, the nonbonded distance between the two helicene termini in the optimized structure of *convex*-**3b** is significantly shortened in *concave*-**3b** (3.294 Å vs 3.061 Å, respectively). Barriers for bowl-to-bowl inversions from the *convex* to the *concave* conformation were also estimated to be 10.6 kcal·mol^{-1} for **3a** and 10.1 kcal·mol^{-1} for **3b**. These values are slightly lower than that for pristine corannulene (~11.5 kcal·mol^{-1}),[3d,e] reflecting the steric influence of the helical motifs on the corannulene motifs during the inversions. The calculations indicate that the *convex* form is the greatly favored conformation and that fast interconversion between the two diastereomeric forms should occur in solution. These conclusions are consistent with the ^{1}H NMR spectra, which exhibit signals for just 16 hydrogens for **3a**, 18 hydrogens for **3b**, and 17 hydrogens for **3c**.

As with the slightly lowered bowl-to-bowl inversion barriers, the calculated helix inversion barriers of **3a** (20.9 kcal·mol^{-1}) and

DOI: 10.1021/acs.orglett.6b01801
Org. Lett. 2016, 18, 3992−3995

3b (34.6 kcal·mol^{-1}) predict easier racemization processes relative to those of pristine [5]helicene (24.1 kcal·mol^{-1})[11] and [6]helicene (36.2 kcal·mol^{-1}),[12] respectively. Conventional transition states with face-to-face oriented terminal rings of the helicene moieties were found for each compound. The curved structures of the corannulene moieties, which resemble the deformations seen in the transition states, help to lower the energetic costs for the helix inversions in **3a** and **3b**.

Enantiomerizations of corannulene−[*n*]helicenes require both of the two inversion motions discussed above. Namely, when starting from the thermodynamically most stable *convex* forms, either one of the inversions of the two flexible motifs, bowl or helix, takes place first to generate a corresponding *concave* form. Then subsequent inversion of the other motif completes the enantiomerization (Figure 3).

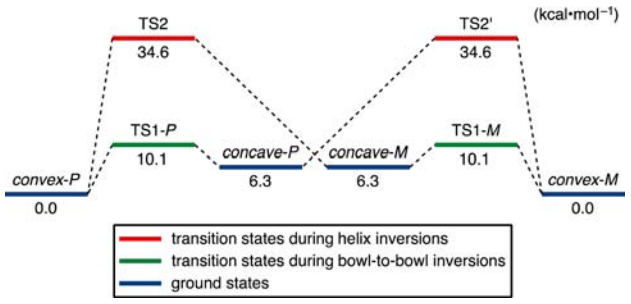

Figure 3. Interconversion pathways of **3b** as a representative of corannulene−[*n*]helicenes. Relative Gibbs free energies (ΔG) were calculated at the B3LYP/6-31G(d) level at 298.15 K and 1 atm. See Figure S6 for the interconversion pathways of **3a**.

Fortunately, optical resolution of *convex*-**3b** was achieved by means of HPLC equipped with a COSMOSIL chlolester column (Figure S3). To the best of our knowledge, this is the first example of a successful separation of enantiomers of a corannulene-based skeletally chiral molecule.[13] With the enantioenriched sample in hand, a kinetic study of the thermal racemization process of *convex*-**3b** in 1,2,4-trichlorobenzene solution was performed by monitoring the decreasing enantiomeric excess (*ee*) by HPLC (Figures S4 and S5). The activation parameters of the helix inversion were experimentally determined to be $\Delta H^{\ddagger} = 31.5$ kcal·mol^{-1} and $\Delta S^{\ddagger} = -6.9$ cal·mol^{-1}·K^{-1}, giving $\Delta G^{\ddagger} = 33.5$ kcal·mol^{-1} at 25 °C. This value is smaller than that for helix inversion of [6]helicene and agrees well with the calculations.

The UV−vis absorption spectrum of **3b** ($CHCl_3$) shows maxima at 418 nm ($\varepsilon = 1.6 \times 10^3$ M^{-1}·cm^{-1}), 315 nm ($\varepsilon = 4.8 \times 10^4$ M^{-1}·cm^{-1}), 289 nm ($\varepsilon = 4.1 \times 10^4$ M^{-1}·cm^{-1}), and 263 nm ($\varepsilon = 6.0 \times 10^4$ M^{-1}·cm^{-1}), with a shoulderlike absorption around 343 nm (Figure 4). The fluorescence maxima appear at 425 and 447 nm ($\Phi_F = 0.06$) (Figure S7). The circular dichroism (CD) spectrum of the faster-eluting peak (>99% *ee*) in the HPLC separation exhibits a positive Cotton effect in the region 300−430 nm ($\Delta\varepsilon^{343\ nm} = +168$ M^{-1}·cm^{-1}) and negative ones below 300 nm ($\Delta\varepsilon^{265\ nm} = -231$ M^{-1}·cm^{-1}). From the CD spectrum simulated by TD-DFT calculations, this faster-moving enantiomer was assigned as *convex-P*-**3b** (Figure S8). The overall CD spectrum is similar but is red-shifted with smaller ellipticity relative to that of *P*-[6]helicene ($\Delta\varepsilon^{324\ nm} = +259$ M^{-1}·cm^{-1} and $\Delta\varepsilon^{246\ nm} = -272$ M^{-1}·cm^{-1}).[14] The specific rotation of *convex-P*-**3b** was also determined to be $[\alpha]_D^{21}$ +4037 ($c = 0.0108$, $CHCl_3$), which is larger than the value $[\alpha]_D^{25}$ +3707 ($c = 0.082$, $CHCl_3$) for *P*-[6]helicene. In contrast to the cases of the hitherto-reported π-extended

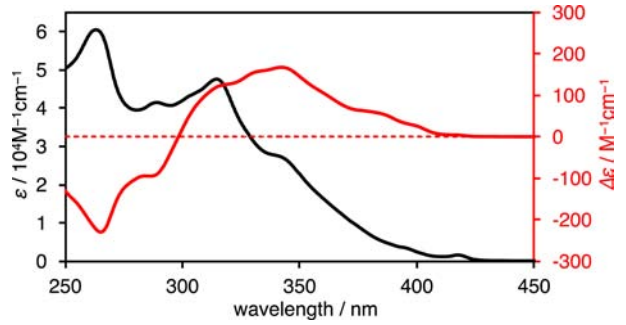

Figure 4. UV−vis absorption (black) and CD (red) spectra of **3b**. The faster-eluting enantiomer was used for the CD measurement.

helicenes, corannulene annulation confers an additional optical rotatory power on the helicene core.[7a,d]

Cyclic voltammetry of **3b** was performed to investigate the electrochemical behavior of the corannulene−[*n*]helicene hybrid π-systems. As in the case of corannulene,[15] **3b** showed an irreversible one-step oxidation wave with a peak potential (E_p) of 1.14 V vs FcH/FcH^+ in acetonitrile. On the other hand, the good electron-accepting ability of corannulene was maintained,[16] and two reversible reduction waves were observed in THF with half-wave potentials ($E_{1/2}$) of −2.35 and −2.65 V vs FcH/FcH^+.

Magnetic shielding effects of the ring currents in corannulenes have previously been reported to move chemical shifts upfield by 2 to 5 ppm.[17] All of these effects, however, were measured over the concave surfaces of corannulenes. The uniquely fixed aromatic rings over the corannulene moiety in our compounds, on the other hand, are suited for probing ring current effects over the convex surface of a geodesic π-system. The ^{1}H NMR signal of the *tert*-butyl group of **3c**, whose *convex* form is also predicted to be favored over the *concave* form by 7.2 kcal·mol^{-1}, is shifted upfield by ca. 0.65 ppm compared with the signal of the *t*-Bu group in **7c** (0.94 vs 1.59 ppm, respectively). Consequently, the *t*-Bu group probe in **3c** provides the first experimental evidence that magnetic shielding over the convex surface of corannulene is not as great as that over the concave surface.

NMR spectral calculations predict chemical shifts of 0.87 ppm for the *t*-Bu group in *convex*-**3c** and −0.06 ppm for that in *concave*-**3c**, as averaged values of the chemical shifts of the nine H atoms in the optimized structures (Figure 5). The sizable difference in these predicted chemical shifts presumably reflects the divergence of the shielding effect on the convex face and the convergence of the shielding effect on the concave face. The good agreement between the experimentally observed chemical shift of the *t*-Bu

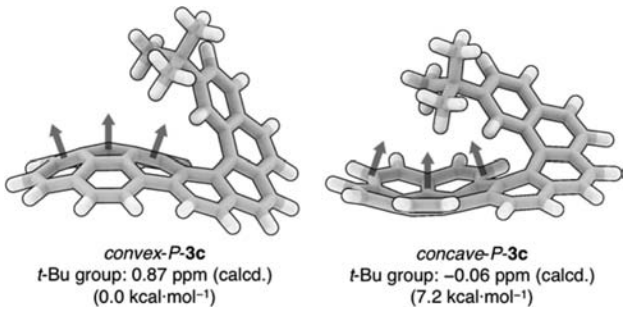

Figure 5. Divergent and convergent shielding effects in the geodesic polycyclic π-systems. ^{1}H NMR chemical shifts were calculated at the B3LYP/6-311+G(2d,p)//B3LYP/6-31G(d) level with $SiMe_4$ (0.0 ppm) as a reference.

DOI: 10.1021/acs.orglett.6b01801
Org. Lett. 2016, 18, 3992−3995

group in **3c** and that calculated for *convex*-**3c** adds further support to the conclusion that the *convex* form predominates not only in the solid state but also in solution.

Compound **3c** is one of the first molecules designed to probe the magnetic environment above the convex surface of corannulene. Following the lead of this NMR study, further studies with other strategically placed groups in helicene moieties could lead to even more interesting results. Similarly, because corannulene can be an aromatic ligand for alkali and transition metals[3a−c,18] and helicenes also can coordinate with metals in a tweezer fashion,[19] properly designed corannulene−[*n*]helicenes could serve as a new type of molecular tweezers with geodesic curvatures by utilizing their intramolecularly proximal π-systems.

The corannulene−[*n*]helicenes provide fundamental insights into a little-explored combination of geodesic curvature and a helical motif. On these characteristic π-systems, the theoretical and experimental studies reveal that the two merged nonplanar motifs, bowl and helix, mutually affect each other's inversion motions, lowering both energetic costs. Optical resolution of the corannulene-based skeletally chiral π-systems was accomplished for the first time, and the influence of bowl annulation on the chiroptical properties of [6]helicene was determined. Additionally, it proved possible to probe the magnetic environment above the convex surface of the corannulene core using the ^{1}H NMR signal of a *tert*-butyl group attached to the helicene moiety.

■ ASSOCIATED CONTENT

Supporting Information

The Supporting Information is available free of charge on the ACS Publications website at DOI: 10.1021/acs.orglett.6b01801.

Experimental procedures and characterization data (PDF)
Crystallographic data for **3b** (CIF)

■ AUTHOR INFORMATION

Corresponding Author

*lawrence.scott@bc.edu

Notes

The authors declare no competing financial interest.

■ ACKNOWLEDGMENTS

This work was supported by the ERATO Program of JST (K.I.), the Funding Program for KAKENHI from MEXT (16K05771 to Y.S.), and the US NSF (CHE-9800711, D.V.P. and L.T.S.). T.F. is a recipient of a JSPS Fellowship for Young Scientists (14J10460). Calculations were performed using the resources of the Research Center for Computational Science, Okazaki, Japan. ITbM is supported by the World Premier International Research Center (WPI) Initiative, Japan.

■ REFERENCES

(1) (a) Barth, W. E.; Lawton, R. G. *J. Am. Chem. Soc.* **1966**, *88*, 380. (b) Lawton, R. G.; Barth, W. E. *J. Am. Chem. Soc.* **1971**, *93*, 1730. (c) Scott, L. T.; Hashemi, M. M.; Meyer, D. T.; Warren, H. B. *J. Am. Chem. Soc.* **1991**, *113*, 7082. (d) Borchardt, A.; Fuchicello, A.; Kilway, K. V.; Baldridge, K. K.; Siegel, J. S. *J. Am. Chem. Soc.* **1992**, *114*, 1921. (e) Scott, L. T.; Cheng, P.-C.; Hashemi, M. M.; Bratcher, M. S.; Meyer, D. T.; Warren, H. B. *J. Am. Chem. Soc.* **1997**, *119*, 10963. (f) Butterfield, A. M.; Gilomen, B.; Siegel, J. S. *Org. Process Res. Dev.* **2012**, *16*, 664.

(2) Reviews of nonplanar π-systems: (a) Rieger, R.; Müllen, K. *J. Phys. Org. Chem.* **2010**, *23*, 315. (b) Dodziuk, H. *Strained Hydrocarbons: Beyond the van't Hoff and Le Bel Hypothesis*; Wiley-VCH: Weinheim, Germany, 2009. (c) Harvey, R. G. *Polycyclic Aromatic Hydrocarbons*; Wiley-VCH: New York, 1997. (d) Pascal, R. A., Jr. *Chem. Rev.* **2006**, *106*, 4809. (e) Tsefrikas, V. M.; Scott, L. T. *Chem. Rev.* **2006**, *106*, 4868. (f) Wu, Y.-T.; Siegel, J. S. *Chem. Rev.* **2006**, *106*, 4843.

(3) (a) Zabula, A. V.; Filatov, A. S.; Spisak, S. N.; Rogachev, A. Y.; Petrukhina, M. A. *Science* **2011**, *333*, 1008. (b) Zabula, A. V.; Spisak, S. N.; Filatov, A. S.; Grigoryants, V. M.; Petrukhina, M. A. *Chem. - Eur. J.* **2012**, *18*, 6476. (c) Ayalon, A.; Rabinovitz, M.; Cheng, P.-C.; Scott, L. T. *Angew. Chem., Int. Ed. Engl.* **1992**, *31*, 1636. (d) Seiders, T. J.; Baldridge, K. K.; Grube, G. H.; Siegel, J. S. *J. Am. Chem. Soc.* **2001**, *123*, 517. (e) Scott, L. T.; Hashemi, M. M.; Bratcher, M. S. *J. Am. Chem. Soc.* **1992**, *114*, 1920. (f) Kavitha, K.; Manoharan, M.; Venuvanalingam, P. *J. Org. Chem.* **2005**, *70*, 2528. (g) Preda, D. V.; Scott, L. T. *Tetrahedron Lett.* **2000**, *41*, 9633.

(4) Yanney, M.; Fronczek, F. R.; Henry, W. P.; Beard, D. J.; Sygula, A. *Eur. J. Org. Chem.* **2011**, *2011*, 6636.

(5) Kawasumi, K.; Zhang, Q.; Segawa, Y.; Scott, L. T.; Itami, K. *Nat. Chem.* **2013**, *5*, 739.

(6) Reviews of helicenes: (a) Shen, Y.; Chen, C.-F. *Chem. Rev.* **2012**, *112*, 1463. (b) Gingras, M. *Chem. Soc. Rev.* **2013**, *42*, 968. (c) Gingras, M.; Félix, G.; Peresutti, R. *Chem. Soc. Rev.* **2013**, *42*, 1007. (d) Gingras, M. *Chem. Soc. Rev.* **2013**, *42*, 1051.

(7) π-Extended helicenes: (a) Buchta, M.; Rybáček, J.; Jančařík, A.; Kudale, A. A.; Buděšínský, M.; Chocholoušová, J. V.; Vacek, J.; Bednárová, L.; Císařová, I.; Bodwell, G. J.; Starý, I.; Stará, I. G. *Chem. - Eur. J.* **2015**, *21*, 8910. (b) Fujikawa, T.; Segawa, Y.; Itami, K. *J. Am. Chem. Soc.* **2015**, *137*, 7763. (c) Bock, H.; Subervie, D.; Mathey, P.; Pradhan, A.; Sarkar, P.; Dechambenoit, P.; Hillard, E. A.; Durola, F. *Org. Lett.* **2014**, *16*, 1546. (d) Jančařík, A.; Rybáček, J.; Cocq, K.; Chocholoušová, J. V.; Vacek, J.; Pohl, R.; Bednárová, L.; Fiedler, P.; Císařová, I.; Stará, I. G.; Starý, I. *Angew. Chem., Int. Ed.* **2013**, *52*, 9970. (e) Bédard, A.-C.; Vlassova, A.; Hernandez-Perez, A. C.; Bessette, A.; Hanan, G. S.; Heuft, M. A.; Collins, S. K. *Chem. - Eur. J.* **2013**, *19*, 16295. (f) Pradhan, A.; Dechambenoit, P.; Bock, H.; Durola, F. *J. Org. Chem.* **2013**, *78*, 2266. (g) Sawada, Y.; Furumi, S.; Takai, A.; Takeuchi, M.; Noguchi, K.; Tanaka, K. *J. Am. Chem. Soc.* **2012**, *134*, 4080. (h) Luo, J.; Xu, X.; Mao, R.; Miao, Q. *J. Am. Chem. Soc.* **2012**, *134*, 13796. (i) Pradhan, A.; Dechambenoit, P.; Bock, H.; Durola, F. *Angew. Chem., Int. Ed.* **2011**, *50*, 12582.

(8) (a) Flammang-Barbieux, M.; Nasielski, J.; Martin, R. H. *Tetrahedron Lett.* **1967**, *8*, 743. (b) Laarhoven, W. H.; Cuppen, Th. J. H. M.; Nivard, R. J. F. *Tetrahedron* **1970**, *26*, 4865. (c) Liu, L.; Yang, B.; Katz, T. J.; Poindexter, M. K. *J. Org. Chem.* **1991**, *56*, 3769.

(9) Petrukhina, M. A.; Andreini, K. W.; Mack, J.; Scott, L. T. *J. Org. Chem.* **2005**, *70*, 5713.

(10) De Rango, C.; Tsoucaris, G.; Delerq, J. P.; Germain, G.; Putzeys, J. P. *Cryst. Struct. Commun.* **1973**, *2*, 189.

(11) Goedicke, Ch.; Stegemeyer, H. *Tetrahedron Lett.* **1970**, *11*, 937.

(12) Martin, R. H.; Marchant, M. J. *Tetrahedron* **1974**, *30*, 347.

(13) Examples of corannulene derivatives with chiral substituents: (a) Kang, J.; Miyajima, D.; Itoh, Y.; Mori, T.; Tanaka, H.; Yamauchi, M.; Inoue, Y.; Harada, S.; Aida, T. *J. Am. Chem. Soc.* **2014**, *136*, 10640. (b) Bandera, D.; Baldridge, K. K.; Linden, A.; Dorta, R.; Siegel, J. S. *Angew. Chem., Int. Ed.* **2011**, *50*, 865.

(14) Nakai, Y.; Mori, T.; Inoue, Y. *J. Phys. Chem. A* **2012**, *116*, 7372.

(15) Janata, J.; Gendell, J.; Ling, C.-Y.; Barth, W.; Backes, L.; Mark, H. B., Jr.; Lawton, R. G. *J. Am. Chem. Soc.* **1967**, *89*, 3056.

(16) Bruno, C.; Benassi, R.; Passalacqua, A.; Paolucci, F.; Fontanesi, C.; Marcaccio, M.; Jackson, E. A.; Scott, L. T. *J. Phys. Chem. B* **2009**, *113*, 1954.

(17) (a) Yanney, M.; Fronczek, F. R.; Sygula, A. *Org. Lett.* **2012**, *14*, 4942. (b) Sygula, A.; Fronczek, F. R.; Sygula, R.; Rabideau, P. W.; Olmstead, M. M. *J. Am. Chem. Soc.* **2007**, *129*, 3842. (c) Seiders, T. J.; Baldridge, K. K.; Siegel, J. S. *Tetrahedron* **2001**, *57*, 3737. (d) Seiders, T. J.; Baldridge, K. K.; Siegel, J. S. *J. Am. Chem. Soc.* **1996**, *118*, 2754.

(18) Petrukhina, M. A.; Scott, L. T. *Dalton Trans.* **2005**, 2969.

(19) Saleh, N.; Shen, C.; Crassous, J. *Chem. Sci.* **2014**, *5*, 3680.

■ NOTE ADDED AFTER ASAP PUBLICATION

The uncorrected version of this paper published on August 4, 2016, the correct version reposted August 5, 2016.

DOI: 10.1021/acs.orglett.6b01801
Org. Lett. 2016, 18, 3992−3995